J Mol Model (2017) 23: 82
DOI 10.1007/s00894-017-3243-x

ORIGINAL PAPER

The influence of Sc doping on structural, electronic and optical properties of $Be_{12}O_{12}$, $Mg_{12}O_{12}$ and $Ca_{12}O_{12}$ nanocages: a DFT study

Masoomeh Omidi[1] · **Hamid Reza Shamlouei**[1] · **Motahareh Noormohammadbeigi**[1]

Received: 2 August 2016 / Accepted: 23 January 2017 / Published online: 17 February 2017

Abstract Density functional theory (DFT) calculations were used to study the effect of scandium doping on the structural, energetic, electronic, linear and nonlinear optical (NLO) properties of $Be_{12}O_{12}$, $Mg_{12}O_{12}$ and $Ca_{12}O_{12}$ nanoclusters. Scandium (Sc) doping on nanoclusters leads to narrowing of their E_g, which enhances their conductance greatly. Also, the polarizability (α) and first hyperpolarizability (β_0) of nanoclusters were dramatically increased as Be, Mg or Ca atoms are substituted with a Sc atom. Among all clusters, α and β_0 values for Sc-doped $Ca_{12}O_{12}$ were the largest. Consequently, the effect of the doping atom, as well as of cluster size, on electronic and optical properties was explored. Time dependent (TD)-DFT calculations were also carried out to confirm the β_0 values; the results show that the higher value of first hyperpolarizability belongs to Sc-doped $Ca_{12}O_{12}$, which has the smallest transition energy (ΔEgn). The results obtained show that these clusters can be candidates for using in electronic devices and NLO materials in industry.

Keywords $X_{12}Y_{12}$ nanocage · DOS · NLO properties · DFT calculation

Introduction

Since the discovery of carbon nanotubes by Ijima [1], the science and technology of nanomaterials has expanded greatly. Due to their unique properties and vast array of different applications, exploring new nanoscale materials has interested many scientists in this field. Many contributions have recently investigated inorganic-based nanomaterials because of their varying characteristics. Using theoretical methods, it was predicted that, among several types of $(XY)_n$ clusters, fullerene-like cages with the general formula of $X_{12}Y_{12}$ would be the most viable [2, 3]. Among $X_{12}Y_{12}$ nanoclusters, metal oxide clusters such as $Be_{12}O_{12}$, $Mg_{12}O_{12}$, and $Ca_{12}O_{12}$ have some remarkable properties due to the significant ionic character of their metal-oxide bonds. Therefore, many efforts have been made to study the physical and chemical properties of above mentioned clusters [4–6]. Recently, Oliveria et al. [7] used quantum chemistry methods to study $Ca_{12}O_{12}$, $Ti_{12}O_{12}$, $Fe_{12}O_{12}$ and $Zn_{12}O_{12}$ nanocage clusters. Their results show that these nanoclusters can be used in catalysis, adsorption processes, gas sensors, and chemical species storage.

Since nonlinear optical (NLO) materials can be used in technological applications such as optical switching, signal processing, information storage, optical communication, laser technology, and in chemical and biological species detection [8, 9], they have attracted great interest. Many studies have been devoted to developing new high-performance NLO materials with potential applications in the fields of optoelectronics and photonics [10–16].

We employed density functional theory (DFT) to adjust the electronic and optical properties of $Be_{12}O_{12}$ and $Mg_{12}O_{12}$ nanoclusters through their interaction with alkali metals, alkali metal superoxides [17–19] and doping with transition metals [20]. In our previous work [20], we doped a $Mg_{12}O_{12}$nanocage with transition metals from the fourth row of the periodic table, and our results indicated that the scandium (Sc) atom has the largest NLO response of all because of its d^1 electronic configuration.

✉ Hamid Reza Shamlouei
shamlouei.ha@lu.ac.ir

[1] Physical Chemistry Group, Chemistry Department, Lorestan University, Khorram Abad, Lorestan, Iran

So, in the present study, applying computational methods based on DFT, we were driven to use the Sc atom with the main aim of enhancing the electronic and NLO response of $Be_{12}O_{12}$, $Mg_{12}O_{12}$ and $Ca_{12}O_{12}$ nanocages.

Computational methods

The geometries of all structures were optimized using the DFT method with the B3LYP/6-31 + G(d) basis set [21, 22]. The B3LYP has proved to be a reliable and commonly used functional method for the study of different nanostructures [23–26]. Frequency calculations were performed at the same level of theory to confirm that all structures are true minima. Since S^2 values were in the range of 0.751–0.752, computational methods were reliable and spin contamination negligible. All calculations were carried out with the Gaussian 09 package [27].

Electronic density of states (DOS) results were obtained using the GaussSum program [28]. The HOMO–LUMO gap (E_g) value, which indicates the electronic properties of each cluster, was calculated as follows:

$$E_g = E_{LUMO} - E_{HOMO} \quad (1)$$

where E_{HOMO} is the energy of highest occupied molecular orbital (HOMO) and E_{LUMO} is the energy of lowest unoccupied molecular orbital (LUMO).

It has been noted that CAM-B3LYP is a suitable approach for exploring NLO properties [29, 30]. So, polarizability(α) and first hyperpolarizability (β_0), which correspond to linear optical and NLO properties, respectively, were calculated by the CAM-B3LYP/6-31 + G(d) method.

In a weak and homogeneous electric field, the molecular energy of systems can be calculated from the following equation [31, 32]:

$$E = E^0 - \mu_\alpha F_\alpha - \frac{1}{2}\alpha_{\alpha\beta}F_\alpha F_\beta - \frac{1}{6}\beta_{\alpha\beta\gamma}F_\alpha F_\beta F_\gamma - \ldots \quad (2)$$

Where E^0 denotes the molecular energy of the system in the absence of an electric field, and F_α is the electric field component along the α direction. μ_α, $\alpha_{\alpha\beta}$ and $\beta_{\alpha\beta\gamma}$ are the tensor components of dipole moment, polarizability, and first hyperpolarizability, respectively. The mean polarizability (α) and magnitude of static first hyperpolarizability (β_0) can be calculated from Eqs. 3 and 4:

$$\alpha = \frac{1}{3}\left(\alpha_{xx} + \alpha_{yy} + \alpha_{zz}\right) \quad (3)$$

$$\beta_0 = \left(\beta_x^2 + \beta_y^2 + \beta_z^2\right)^{1/2} \quad (4)$$

In which

$$\beta_I = \frac{3}{5}\left(\beta_{iii} + \beta_{ijj} + \beta_{ikk}\right) \quad i,j,k = x,y,z. \quad (5)$$

where β_{ijk} (i, j, k = x, y, z) are the components of the first hyperpolarizability tensor. The relation between hyperpolarizibility and other time-dependent properties were calculated using the two-level model [33–35] described by Eq. 6:

$$\beta_0 \propto \frac{f_0 \Delta\mu}{\Delta E^3} \quad (6)$$

where ΔE , f_0 and $\Delta\mu$ are the transition energy, oscillator strength, and difference in the dipole moments between the ground state and the crucial excited state, respectively. In the proposed model, β is proportional to ΔE^3, and so ΔE is the critical factor in the first hyperpolarizability [36–38].

Due to the dependence of the first hyperpolarizability on ground state and excited states properties, time-dependent density functional theory (TD-DFT) calculations at CAM-B3LYP/6-31 + G(d) level of theory were performed to obtain the excitation energy and the differences of their dipole moments between the ground state and excited state as well as oscillator strength f_0.

Results and discussion

Structural optimization

The optimized structures and geometry parameters of the $Be_{12}O_{12}$, $Mg_{12}O_{12}$ and $Ca_{12}O_{12}$ nanocages are depicted in Fig. 1. Each cluster consists of six square and eight hexagonal rings. The X–O and X–X (X refers to Be, Mg and Ca in pristine $Be_{12}O_{12}$, $Mg_{12}O_{12}$ and $Ca_{12}O_{12}$, respectively) bond lengths in square rings were analyzed, and the results are gathered in Table 1. The Be–O, Mg–O, and Ca–O bond lengths are equal to 1.58, 1.95, and 2.28 Å, and Be–Be, Mg–Mg, and Ca–Ca bond length values are 2.06, 2.68, and 3.24 Å, respectively. The order of calculated bond lengths is in accordance with the radii of metal atoms.

The Be, Mg, and Ca atoms were then substituted by a scandium atom in the corresponding cages, the fully optimized structures of which are presented in Fig. 1. As can be seen in Fig 1, the structures of the nanocages were moderately distorted, and bond lengths and angles were modified by doping a Sc atom in the cage. In the optimized Sc-doped $Be_{12}O_{12}$, the Sc atom impurity is projected out of the cage surface in order to reduce stress due to its larger size compared to the Be atom. The Be–O distance in pristine $Be_{12}O_{12}$ is 1.58 Å, which increases to 2.03 Å for the Sc–O bond in $Be_{11}ScO_{12}$. As a result of Sc doping, the Mg–O distance changed from 1.95 Å to 1.97 Å in the $Mg_{11}ScO_{12}$ nanocluster, which is the smallest bond length change compared to other nanocages. For $Ca_{12}O_{12}$, the nanocage Ca–O bond length is 2.28 Å, which

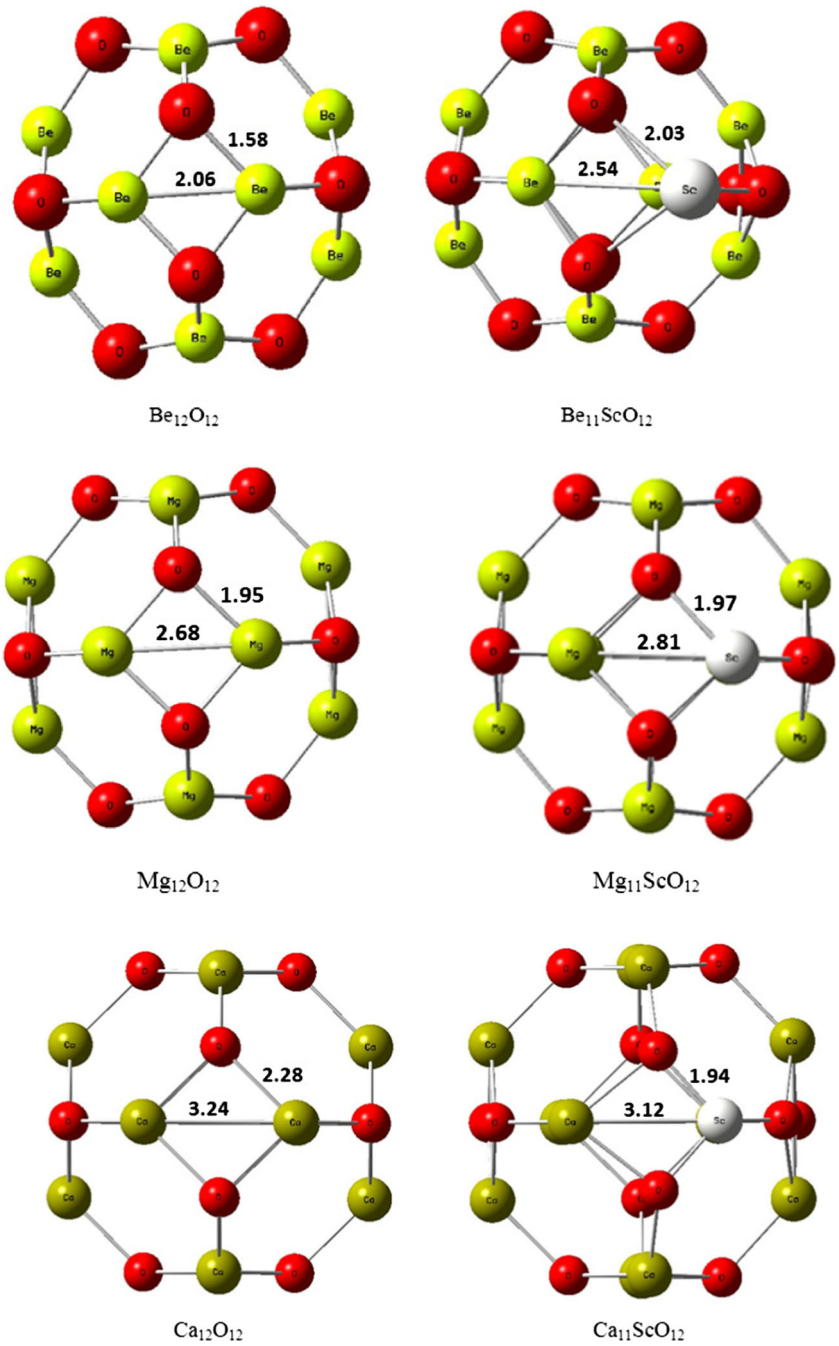

$Be_{12}O_{12}$ $Be_{11}ScO_{12}$ $Mg_{12}O_{12}$ $Mg_{11}ScO_{12}$ $Ca_{12}O_{12}$ $Ca_{11}ScO_{12}$

Fig 1 Optimized structures of pristine and Sc-doped $Be_{12}O_{12}$, $Mg_{12}O_{12}$ and $Ca_{12}O_{12}$ nanocages

Table 1 X–O (compared with previous reports) and X–X bond length (Ångstrom), O–X–O bond angle (degree) and E_{dop} (kcal mol^{-1}) for pristine and Sc-doped $Be_{12}O_{12}$, $Mg_{12}O_{12}$ and $Ca_{12}O_{12}$ nanoclusters [the X in pristine metal oxide relates to metals (Be, Mg and Ca), but in Sc-doped nanocages, correspond to Sc atom]

System	X–O	X–O (previous reports)	X–(Be, Mg, Ca)	O–X–O	E_{dop}
$Be_{12}O_{12}$	1.58	1.584 [17], 1.58 [18]	2.06	98.13	—
$Be_{11}ScO_{12}$	2.03	–	2.54	77.37	8.93
$Mg_{12}O_{12}$	1.95	1.953 [17], 1.95 [19, 20]	2.68	92.96	—
$Mg_{11}ScO_{12}$	1.97	1.970 [20]	2.81	89.15	−72.95
$Ca_{12}O_{12}$	2.28	2.19 [7]	3.24	89.36	—
$Ca_{11}ScO_{12}$	1.94	–	3.12	96.79	−95.81

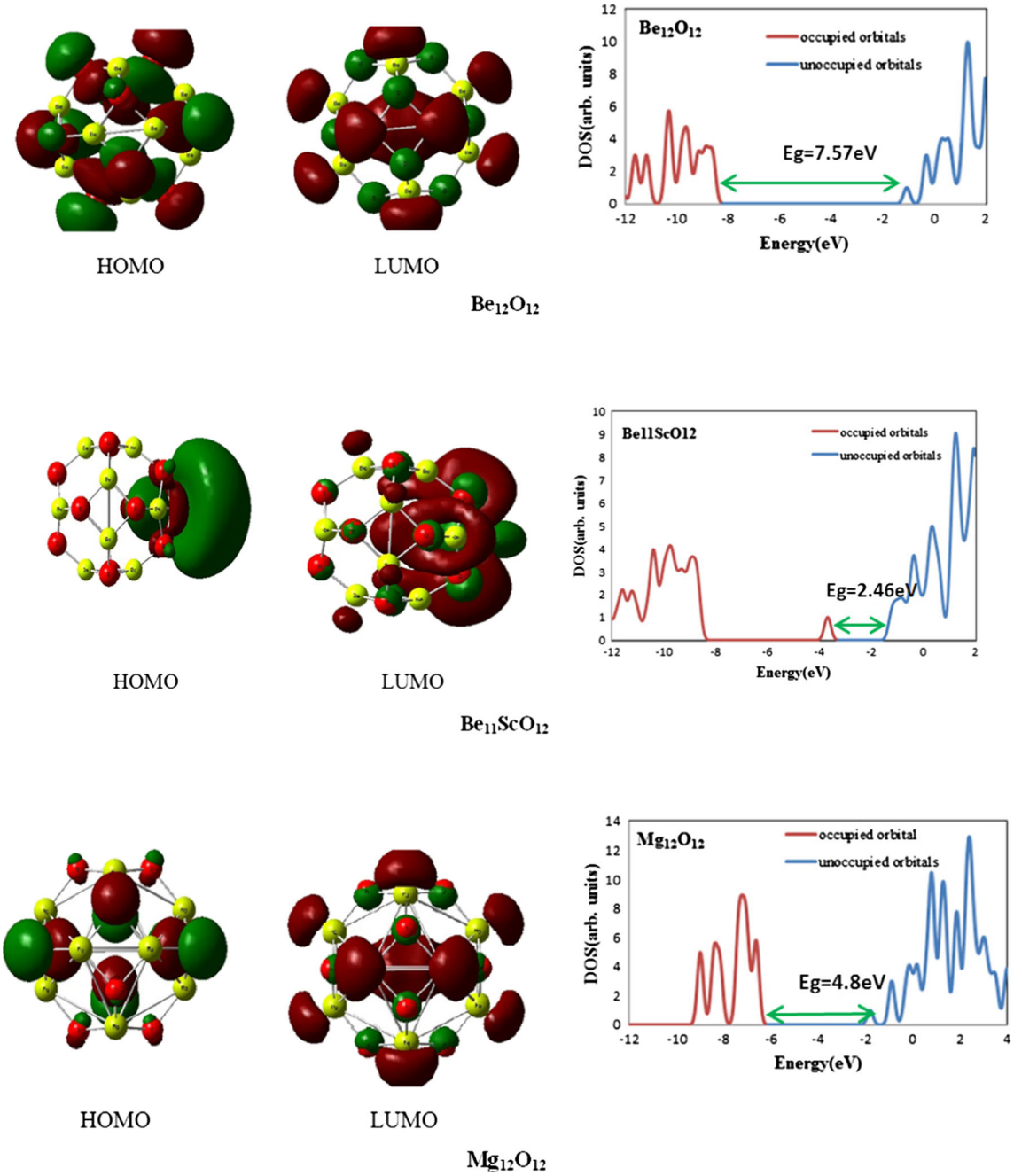

Fig 2 Highest occupied molecular orbital (HOMO)–lowest unoccupied molecular orbital (LUMO) distribution and density of states (DOS) plots for all considered nanocages

decreases to 1.94 Å by Sc doping. So the deformation of $Be_{12}O_{12}$ was greater than that of the other cages because the size difference of Sc to Be is greater than its difference to Mg and Ca. Additionally, as a consequence of Sc doping, enlarged bond length was seen for $Be_{12}O_{12}$ and $Mg_{12}O_{12}$, and decreased bond length was observed for the $Ca_{12}O_{12}$ nanocluster. Also, doping the scandium atom in nanoclusters affected the X–O–X angle and, as reported in Table 1, the angle for $Be_{12}O_{12}$ and $Mg_{12}O_{12}$ decreased while that in $Ca_{12}O_{12}$ increased.

Doping energy (E_{dop}), the energy required for substituting a Be, Mg or Ca atom with a Sc atom, can be calculated from Eq. 7:

$$E_{dop} = E[X_{11}ScO_{12}] + E[X] - E[X_{12}O_{12}] - E[Sc] \quad (7)$$

where $E[X_{12}O_{12}]$ and $E[X_{11}ScO_{12}]$ refer to the energy of pristine and Sc-doped nanoclusters, and $E[X]$ and $E[Sc]$ are the energy of an isolated Be/Mg/Ca and Sc atom, respectively.

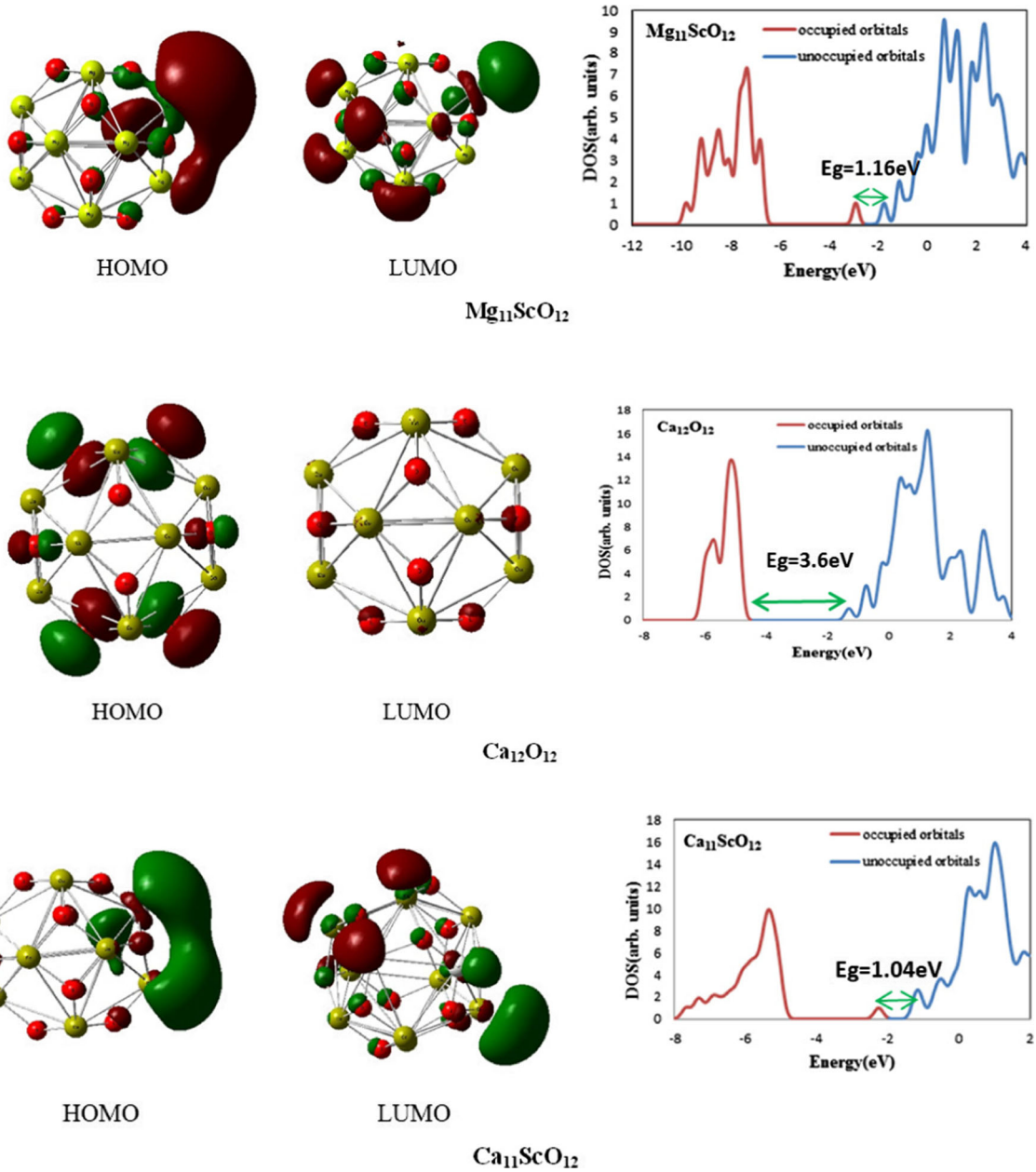

Fig. 2 (continued)

The values of calculated E_{dop} for Sc-doped nanocages are listed in Table 1. The $Mg_{12}O_{12}$ and $Ca_{12}O_{12}$ had a partially negative value of doping energy (−72.95 kcal mol^{-1} for $Mg_{12}O_{12}$and −95.81 kcal mol^{-1} for $Ca_{12}O_{12}$), whereas the $Be_{12}O_{12}$ nanocluster had a positive value of doping energy equal to 8.93 kcal mol^{-1}. These results may be due to the greater size difference of Sc to Be than its difference to Mg and Ca. From optimizing the structure and carrying out the frequency test, it is obvious that the $Be_{11}ScO_{12}$ is a stable compound that can be employed in a dipole moment, polarizability and hyperpolarizability study. But formation of $Be_{11}ScO_{12}$ from direct doping of the free Sc atom, which is the meaning of doping energy, is an energy-consuming process. It is evident that a different raw material must be used to produce $Be_{11}ScO_{12}$, or that a kinetic control mechanism must be used rather than an equilibrium control mechanism.

Electronic properties

We next investigated the effect of Sc doping on the electronic properties of $Be_{12}O_{12}$, $Mg_{12}O_{12}$ and $Ca_{12}O_{12}$ nanoclusters. The HOMO–LUMO distribution and density of states (DOS) plots for all considered nanocages are presented in Fig. 2. As shown in Fig. 2, for pristine nanoclusters, the HOMO is concentrated over the oxygen atoms of the cage, while the LUMO is spread over the Be, Mg and Ca atoms.

Table 2 Frontier molecular orbital energies (E_H and E_L), HOMO–LUMO gap (E_g) (compared with previous reports) and the percent of ΔEg values obtained for pristine and Sc-doped $Be_{12}O_{12}$, $Mg_{12}O_{12}$ and $Ca_{12}O_{12}$nanoclusters

System	E_H(eV)	E_L(eV)	E_g (eV)	E_g (previous reports)	%ΔEg
$Be_{12}O_{12}$	−8.62	−1.05	7.57	7.550 [17], 7.60 [18]	—
$Be_{11}ScO_{12}$	−3.69	−1.23	2.46	–	−67.50
$Mg_{12}O_{12}$	−6.6	−1.8	4.80	4.794 [17], 4.80 [19, 20]	—
$Mg_{11}ScO_{12}$	−2.92	−1.76	1.16	1.16 [20]	−75.83
$Ca_{12}O_{12}$	−4.9	−1.3	3.60	4.0 [7]	—
$Ca_{11}ScO_{12}$	−2.26	−1.22	1.04	–	−71.11

The energies of the HOMO and LUMO, and subsequent energy gap (E_g), were evaluated from the DOS spectra and Eq 1 summarized in Table 2. The E_g values of pristine $Be_{12}O_{12}$, $Mg_{12}O_{12}$ and $Ca_{12}O_{12}$ are about 7.57 kcal mol^{-1}, 4.8 kcal mol^{-1} and 3.6 kcal mol^{-1} respectively. These E_g values are in accordance with the previous reports [7, 39, 40], and indicate that these nanocages are semiconductor materials. Moreover, it is obvious from Table 2 that doping a scandium atom on the nanocages leads to significant narrowing of the E_g, and this narrowing is almost the same for all cages (the percent of ΔE_g for Sc-doped $Be_{12}O_{12}$, $Mg_{12}O_{12}$ and $Ca_{12}O_{12}$ is equal to −67.50, −75.83, and −71.11, respectively), which shows that the amount of E_g narrowing is due to Sc atom nature rather than cluster size. So, in the presence of the scandium atom, the electronic conductance of all cages increases. The E_g values for Sc-doped $Be_{12}O_{12}$, $Mg_{12}O_{12}$ and $Ca_{12}O_{12}$ are equal to 2.46 kcal mol^{-1}, 1.16 kcal mol^{-1}, and 1.04 kcal mol^{-1}, respectively. As illustrated in Fig. 2, it is apparent that doping Sc atom on the clusters releases electron charge on the nanocluster, and causes the formation of a high energy level at a new HOMO level located between the original HOMO and LUMO of pristine nanocages. This new HOMO level may be responsible for the significant narrowing of E_g values.

To indicate the orientation of Sc-doped $Be_{12}O_{12}$, $Mg_{12}O_{12}$ and $Ca_{12}O_{12}$ nanoclusters in an electric field, their molecular electrostatic potential surface was plotted, as depicted in Fig 3.

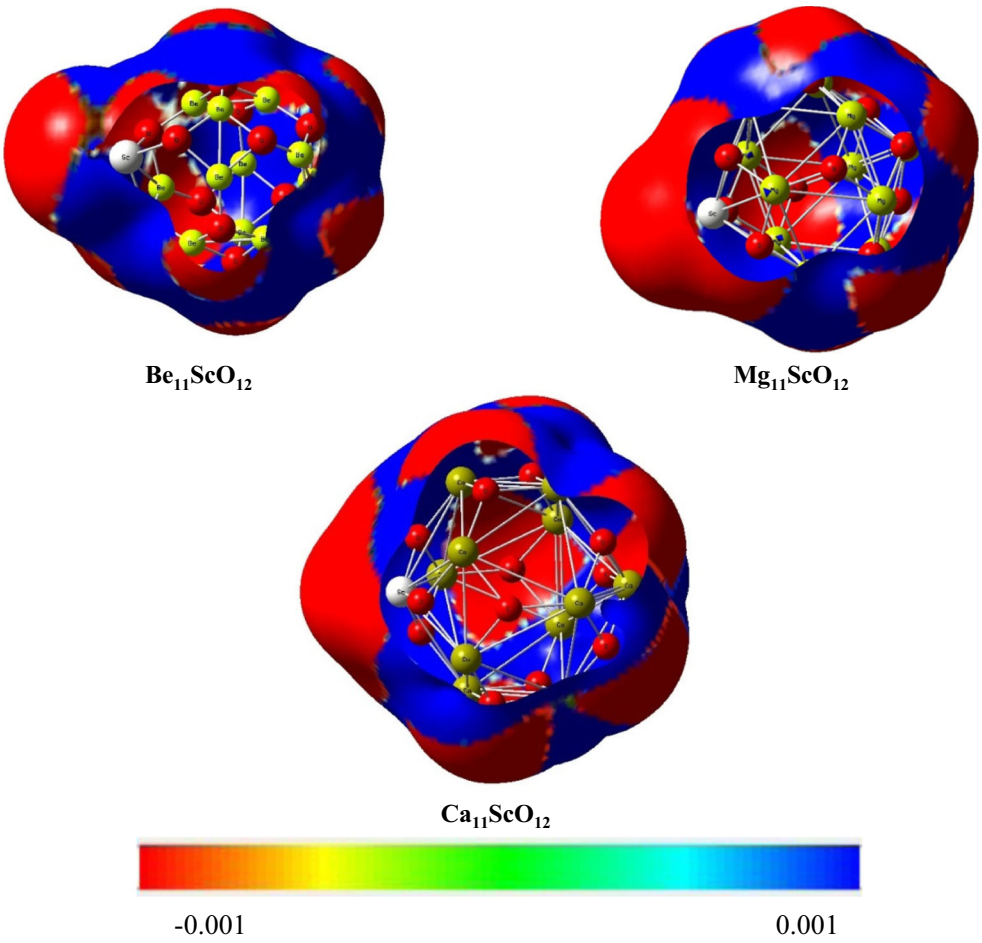

Fig 3 Molecular electrostatic potential surface of the Sc doped $Be_{12}O_{12}$, $Mg_{12}O_{12}$ and $Ca_{12}O_{12}$nanocages. The surfaces are defined by the 0.001 electrons/b3 contour of the electronic density. Color ranges in a.u.

Table 3 Polarizability (α), hyperpolarizability (β_0) and dipole moment (μ) values for pristine and Sc-doped nanoclusters

System	β_0(a.u.)	α (a.u.)	μ (Debye)
$Be_{12}O_{12}$	0.03	127.60	0.00
$Be_{11}ScO_{12}$	4953.06	187.24	1.49
$Mg_{12}O12$	0.2	215.4	0.00
$Mg_{11}ScO_{12}$	47,871.67	365.23	4.64
$Ca_{12}O_{12}$	7.23	311.6	0.01
$Ca_{11}ScO_{12}$	298,786.51	1065.95	7.09

In Fig. 3, the locations of the various most positive and most negative regions were shown by the molecular electrostatic potential surface. It is obvious from Fig. 3 that the electron density was concentrated mainly over the scandium head of the molecules, therefore, in an electric field, the scandium head was oriented toward the positive pole.

Optical properties

Polarizability(α) and first hyperpolarizability(β_0), which denote linear and NLO properties, were calculated, and the results are listed in Table 3. Calculated α values for pristine $Be_{12}O_{12}$, $Mg_{12}O_{12}$ and $Ca_{12}O_{12}$ are about 127.6, 215.4 and 311.6, respectively, increasing to 187.24, 365.23 and 1065.95, respectively, for Sc-doped corresponding nanoclusters. The obtained values of first hyperpolarizability (β_0) for pristine $Be_{12}O_{12}$, $Mg_{12}O_{12}$ and $Ca_{12}O_{12}$ are equal to 0.03, 0.2 and 7.23 a.u. (atomic unit). respectively. and these values increase significantly with doping a scandium atom on nanoclusters. (The β_0 values for Sc-doped $Be_{12}O_{12}$, $Mg_{12}O_{12}$ and $Ca_{12}O_{12}$ are about 4953.06, 47,871.67 and 298,786.51 a.u., respectively.) These results show that doping of nanoclusters with a scandium atom leads to an enormous increment in α and β_0. Therefore, an effective approach to enhance the NLO response of these metal oxide nanoclusters is to dope them with a scandium atom.

Table 4 Time-dependent (TD)-CAM-B3LYP/6-31 + g(d) calculated results of transition energy ($\Delta E_{g\text{-}n}$), transition moment ($\mu_{g\text{-}n}$), oscillator strength ($f_{g\text{-}n}$) and the major electric transition (CT) for all nanoclusters

System	ΔE (ev)	Δμg-e (a.u.)	f_0 (a.u.)	S^2	CT[a]
$Be_{12}O_{12}$	7.51	0.00	0.005	0.000	H-4 → L + 2
$Be_{11}ScO_{12}$	3.12	0.79	0.089	0.752	H → L
$Mg_{12}O_{12}$	4.86	0.00	0.008	0.000	H-4 → L + 2
$Mg_{11}ScO_{12}$	1.49	2.53	0.117	0.751	H → L
$Ca_{12}O_{12}$	3.71	0.16	0.014	0.000	H-12 → L + 3
$Ca_{11}ScO_{12}$	0.88	3.25	0.211	0.751	H → L + 2

[a] H and L refer to the HOMO and LUMO, respectively

The data in Table 3 show that the magnitude of the Sc doping effect on polarizability and first hyperpolarizability depends significantly on the size of nanocluster, and that the doping effect on these properties seriously increases with increasing the size of the nanocluster.

Time-dependent density functional theory

Time-dependent density functional theory (TD-DFT) calculations at the CAM-B3LYP/6-31 + G(d) level of theory was used to obtain transition excited state properties such as excitation energies E(eV), oscillator strengths *f* (a.u.), major electric transition (CT), and transition moment of all configurations listed in Table 4.

As presented in Eq. 6, β_0 is a function of the variables reported in Table 4. So the TD-DFT calculations prove the β_0 values obtained above. Based on data presented in Tables 3 and 4, it is obvious that the excitation energy has an inverse relationship to the hyperpolarizibility values. A drastic change in hyperpolarizability (with inverse of 3 powers) occurs, with a small change in transition energy. The Sc-doped $Ca_{12}O_{12}$ nanocage has the smallest transition energy (ΔEgn), which corresponds to highest value of hyperpolarizability (β_0).

Conclusions

The influence of scandium doping on the structural, energetic, electronic and optical properties of $Be_{12}O_{12}$, $Mg_{12}O_{12}$ and $Ca_{12}O_{12}$ was investigated using DFT calculations at B3LYP/6-31 + g(d) level of theory. The results can be summarized as follows:

(1) The Sc doping effect on nanocluster optical properties depends on both nature of doped atom and size of nanoclusters.
(2) The E_g values of nanoclusters narrowed drastically upon scandium doping, and this narrowing was almost the same for all cages and is due to the nature of the Sc atom not the cluster size.
(3) Doping of scandium on $Be_{12}O_{12}$, $Mg_{12}O_{12}$ and $Ca_{12}O_{12}$ nanoclusters increases their dipole moment.
(4) The values of polarizability and first hyperpolarizability are enhanced as the Be, Mg or Ca atoms are replaced with a scandium atom, and the largest increment in β_0 occurred on Sc-doped $Ca_{12}O_{12}$.
(5) TD-DFT results indicate that the Sc-doped $Ca_{12}O_{12}$ nanocage, having the smallest value of transition energy ($\Delta E_{g\text{-}n}$), has the largest value of first hyperpolarizability.

Acknowledgements We are very thankful to Dr. Hossein Farrokhpour in Isfahan University of Technology for providing the Gaussian 09 Package.

References

1. Ijima S (1991) Nature 354:56–58
2. Strout DL (2000) J PhysChem A 104:3364–3366
3. Wang R, Zhang D, Liu C (2005) Chem Phys Lett 411:333–338
4. Chen L, Zhou GQ, Xu C, Zhao T, Huo Y (2009) J Mol Struct Theochem 900:33–36
5. Haertelt M, Fielicke A, Meijer G, Kwapien K, Sierka M, Sauer J (2012) Phys Chem Chem Phys 14:2849–2856
6. Kwapien K, Sierka M, Dobler J, Sauer J, Haertelt M, Fielicke A, Meijer G (2011) Angew Chem Int Ed 50:1716–1719
7. Oliveira OV, Pires JM, Neto AC, Santos JD (2015) Chem Phys Lett 634:25–28
8. Sagadevan S, Varatharajan R (2013) Mater Phys Mech 18:11–17
9. Wang Y, Xie X, Goodson T (2005) Nano Lett 5:2379–2348
10. Zhong RL, Xu HL, Muhammad S, Zhang J, Su ZM (2012) J Mater Chem 22:2196–2202
11. Tu C, Yu G, Yang G, Zhao X, Chen W, Lia S, Huang X (2014) Phys Chem Chem Phys 16:1597–1606
12. Zhou ZJ, Yu GT, Ma F, Huang XR, Wu ZJ, Li ZR (2014) J Mater Chem C 2:306–311
13. Hatua K, Nandi PK (2013) J Phys Chem A 117:12581–12589
14. Muhammad S, Xu H, Su Z (2011) J Phys Chem A 115:923–931
15. Ma F, Miao T, Zhongjun Z, Sun D (2013) J Mol Model 19:4805–4813
16. Wang J, Wang WY, Fang XY, Qiu YQ (2015) J Mol Model 21:95
17. Shakerzdeh E, Tahmasebi E, Shamlouei HR (2015) SYNTHETIC MET 204:17–24
18. RaoofToosi A, Shamlouei HR, Mohammadi Hesari A (2016) Chin Phys B 25:094220–1
19. Mohammadi Hesari A, Shamlouei HR, Raoof Toosi A (2016) J Mol Model 22:189
20. Shamlouei HR, Nouri A, Mohammadi A, DadkhahTehrani A (2016) Phys E Low Dimens Syst Nanostruct 77:48–53
21. Becke AD (1988) Phys Rev A 38:3098
22. Lee C, Yang W, Parr RG (1988) Phys Rev B 37:785–789
23. Ahmadi A, Hadipour NL, Kamfiroozi M, Bagheri Z (2012) Sensors Actuators B 161:1025–1029
24. Beheshtian J, Peyghan AA, Bagheri Z (2012) Comp Mater Sci 62: 71–74
25. Beheshtian J, Kamfiroozi M, Bagheri Z, Ahmadi A (2011) Phys E 44:546–549
26. Beheshtian J, Peyghan AA, Bagheri Z (2012) Sensors Actuators B 171–172:846–852
27. Frisch MJ, Trucks GW, Schlegel HB et al (2009) Gaussian 09, revision A.1. Gaussian, Inc, Wallingford
28. O'Boyle N, Tenderholt A, Langner K (2008) J Comput Chem 29: 839–845
29. Yanai T, Tew D, Handy N (2004) Chem Phys Lett 393:51–57
30. Janjua MRSA, Jamil S, Ahmad T, Yanga Z, Mahmood A, Pan S (2014) Comput Theor Chem 1033:6–13
31. Buckingham AD (1967) Adv Chem Phys 12:107–142
32. McLean AD, Yoshimine M (1967) J Chem Phys 47:1927–1935
33. Oudar JL, Chemla DS (1977) Chem Phys 66:2664
34. Oudar JL (1977) Chem Phys 67:446
35. Kanis DR, Ratern MA, Marks TJ (1994) Chem Rev 94:195
36. Ayan D, Swapan KP (2006) Chem Soc Rev 35:1305
37. Parr RG, Yang W (1993) Int J Quantum Chem 47:101
38. Koopmans TA (1934) Physica 1:104
39. Shakerzadeh E, Inorg J (2014) Organomet Polym 24:694–705
40. Chen L, Xu C, Zhang X, Cheng C, Zhou T (2009) Phys E Low Dimens Syst Nanostruct 41:852–855